Aalto University
School of Science
Degree programme in Engineering Physics and Mathematics

Methods for Removing Digital Image Noise by Merging Multiple Exposures

Bachelor's Thesis
19.8.2019

Viljami Uusihärkälä

The document can be stored and made available to the public on the open internet pages of Aalto University.
All other rights are reserved.

Aalto University
School of Science

Aalto University, P.O. BOX 11000, 00076 AALTO
www.aalto.fi

Abstract of bachelor's thesis

Author Viljami Uusihärkälä

Title of thesis Methods for Removing Digital Image Noise by Merging Multiple Exposures

Degree programme Engineering Physics and Mathematics

Major Mathematics and Systems Sciences **Code of major** SCI3029

Supervisor Asst.Prof. Pauliina Ilmonen

Thesis advisor(s) D.Sc. Lauri Viitasaari

Date 19.8.2019 **Number of pages** 25 **Language** English

Abstract

Digital imaging is constantly growing and is being applied into various new fields of technology. While digital image sensors are improving every day, they still involve digital noise in the obtained images. Many applications, including photography, require the use of noiseless images for better results. Thus it is of great importance to have variety of powerful noise reduction methods available. Whereas most techniques concentrate on removing noise from single image file, it is possible to utilize information from several images in order to acquire noise-free image. In this thesis, we focus on noise reduction methods that merges together information from multiple exposures of the same stationary subject.

The introduced merging methods (average and median based) are compared to more conventional single-image denoising techniques. In order to analyze the performance of the methods, a total of 252 images were captured using a regular consumer DSLR camera. Due to the requirements of merging methods, the images were taken such that the consecutive exposures would be identical, excluding the noise. The effectiveness of the methods is compared using pixel variance as a measure of noise. In addition to the variance in the processed images, visual effects of methods are also considered, since noise is essentially visual aberration of the subject.

The results propose strong applicability of both merging methods. That is, both of the methods were able to significantly reduce the pixel variance in the test images, indicating apparent reduction in the noise. The visual comparisons of the methods illustrated the advantages of merging methods in noise reduction, as the merging methods outperformed the conventional ones in terms of edge and feature preservation. The merging methods even sharpened the test images, which is an important property in many noise reduction applications, such as medical imaging.

Keywords noise reduction, image processing, image averaging, noise model, Gaussian noise, pixel variance

Aalto-yliopisto
Perustieteiden korkeakoulu

Aalto-yliopisto, PL 11000, 00076 AALTO
www.aalto.fi
Tekniikan kandidaatintyön tiivistelmä

Tekijä Viljami Uusihärkälä

Työn nimi Methods for Removing Digital Image Noise by Merging Multiple Exposures

Koulutusohjelma Teknillinen fysiikka ja matematiikka

Pääaine Matematiikka ja systeemitieteet **Pääaineen koodi** SCI3029

Vastuuopettaja Apulaisprofessori Pauliina Ilmonen

Työn ohjaaja(t) TkT. Lauri Viitasaari

Päivämäärä 19.8.2019 **Sivumäärä** 25 **Kieli** englanti

Tiivistelmä

Digitaalinen valokuvaaminen ja kuvantaminen on alati kasvava ala, jota hyödynnetään yhä laajemmin uusissa teknologian käyttökohteissa. Nopeasta kehityksestä huolimatta digitaalisilla kennoilla otetuissa kuvissa esiintyy edelleen digitaalista kohinaa, eli satunnaista vaihtelua signaalissa. Perinteisen valokuvauksen lisäksi monet sovellusalat vaativat käyttöönsä lähes kohinavapaita kuvia, mikä luo tarpeen tehokkaille kohinanpoistomenetelmille. Perinteisesti kohinanpoistomenetelmät pyrkivät vähentämään kohinaa yksittäisistä kuvista, mutta kohinavapaan kuvan aikaansaamiseksi on myös mahdollista hyödyntää useampaa kuvaa. Tässä tutkielmassa keskitytään menetelmiin, jotka hyödyntävät useammasta samanlaisesta kuvasta saatua lisäinformaatiota yhden kohinavapaan kuvan luomiseksi.

Tutkielmassa käsiteltävät menetelmät perustuvat useamman kuvan yhdistämiseen keskiarvon ja mediaanin avulla. Näitä yhdistelymenetelmiä verrataan tavanomaisempiin yhden kuvan kohinanpoistomenetelmiin. Jotta esiteltyjä menetelmiä voitaisiin vertailla, työtä varten otettiin 252 valokuvaa käyttäen tavanomaista järjestelmäkameraa. Kuvia yhdistelevien metodien luonteesta johtuen kuvat otettiin siten, että ne eroaisivat toisistaan vain kohinan verran. Kohinanpoistomenetelmien toimivuutta vertailtiin tarkastelemalla käsiteltyjen kuvien pikseleiden välistä varianssia, mikä antaa käsityksen kohinan määrästä. Koska digitaalinen kohina on lopulta vain kuvan vääristymää, tarkasteltiin myös menetelmien silminnähtävää paremmuutta.

Tutkielman tulokset osoittavat yhdistelymenetelmien olevan tehokkaita kohinanpoistomenetelmiä. Molemmat tutkitut menetelmät onnistuivat pienentämään pikseleiden varianssia, mikä tarkoittaa lopullisen kohinan vähenemistä. Myös silmämääräisissä vertailuissa yhdistelymenetelmät osoittautuivat tavanomaisia metodeja paremmiksi, pystyessään säilyttämään enemmän informaatiota, kuten reunoja ja muita ominaisuuksia. Yhdistelymenetelmät jopa paransivat alkuperäisten kuvien tarkkuutta, mikä tekee niistä varteenotettavan vaihtoehdon monissa sovelluksissa, kuten lääketieteellisessä kuvantamisessa.

Avainsanat kohinanpoisto, kuvankäsittely, keskiarvomenetelmä, kohinamalli, Gaussinen kohina, pikselin varianssi

Contents

1 Introduction

Digital image sensors have revolutionized photography and its applications in the past decade. The growth of digital imaging tends to increase as sensor technology develops and digital cameras are being applied into more various types of technological applications.

Digital camera sensors are essentially photon counting devices which are not ideal by any means. In fact, all digital images captured by a digital sensor contain some degree of noise. Noise is random degradation in an image that can be caused by a number of different sources. As noise always reduces the amount of information provided by the image, noise is usually unwanted phenomenon which is desired to be removed [1].

Noise can be removed in various different ways. Some methods use linear filtering across the whole image, while others take advantage of non-linear operations, such as low pass filtering, in order to denoise the image [14]. Whereas the aforementioned methods apply the denoising into one single image, it is possible to take advantage of several exposures while attempting to obtain a noiseless image [3].

In this thesis, we concentrate on denoising methods that make use of consecutive exposures. These multi-image denoising methods have some major advantages compared with the more traditional single-image denoising techniques [3]. On the other hand, multi-image methods are practical in very few situations. Multi-image methods can be practical when the frames are registered and the photographed subject remains stationary [1, 6]. Despite the restrictions, multiple stationary exposures can be taken for noise reduction purposes in fields such as medical imaging or astrophotography [15]. Our objective is to compare these image merging methods to more conventional alternatives, by means of variance as well as visual properties of the processed images.

2 Digital image noise

2.1 Noise models

It is usually beneficial to have prior knowledge of the underlying model of the noise, before it can be removed. Therefore, noise can be divided into different models based on its source and mathematical form. As noise is typically

caused by numerous different sources, it can be very diverse. Noise is often emerged during the image digitization by altering light levels and high sensor temperature, both of which cause variations in the signal. Transmission is another part where noise is produced. Usually, the signal interferes in the channel which can cause noise in the final image as well [4].

A noisy image, $g(x, y)$, can be decomposed into two components: the underlying real image $f(x, y)$ and the added noise $n(x, y)$, where (x, y) corresponds to the spatial coordinates of the image. This decomposition is written as

$$g(x, y) = f(x, y) + n(x, y). \tag{1}$$

The decomposition is often referred to as an additive model, which is used in companion with many other noise models [3]. Most noise models assume that the noise is uncorrelated with the image. This means that the noise values $n(x, y)$ cannot depend on the real values of $f(x, y)$. Another assumption is that noise is independent of spatial coordinates, (x, y), across the whole image area. In this section we introduce yet two more noise models, which are relatively common in traditional photography that uses CMOS-sensors. These noise models are called Gaussian noise and Salt and Pepper noise, respectively.

The Gaussian noise model is the most used in practice, since it models real noise well and it is mathematically very pleasing. Gaussian noise is used to model noise that arises from electric circuit and sensor, which are one of the most significant components to contribute to the final noise in the image. Gaussian model explains the noise the better the higher the sensor temperature is during the exposure and the weaker the lighting is. Gaussian is very well modeled with the additive model in Equation (1), where each noise component $n(x, y)$ is normally distributed [3]. That is, each noise component $n(x, y)$ follow the normal distribution with mean μ and standard deviation σ. The probability density function is given by

$$p(n) = (2\pi\sigma^2)^{-1/2} e^{-(n-\mu)^2/2\sigma^2}. \tag{2}$$

In Equation (2), n corresponds to the gray level value of the noise component $n(x, y)$. Furthermore, in the context of the additive model, the mean of the Gaussian noise is zero, that is $\mu = 0$.

Another common, but not so visually apparent, noise model is the Salt and Pepper noise. Salt and Pepper noise is typically caused by errors in data

transmission in camera. The errors may be caused by faulty image sensor or damaged memory. Since data is stored in bit form in the camera, Salt and Pepper noise is usually 0-1 noise. That is, Salt and Pepper noise degrade the image by adding minimum and maximum gray scale values in the image, most often values 0 and 255, as images are usually stored in 8-bit format. Due to this behaviour, Salt and Pepper noise cannot be modeled with the additive model. It is common that various types of noise occur simultaneously in images. Therefore, Gaussian and Salt and Pepper can be observed concurrently. The probability density function of Salt and Pepper is given in Equation (3).

$$\begin{aligned} p(g = f) &= 1 - \alpha, \\ p(g = max) &= \alpha/2, \\ p(g = min) &= \alpha/2 \end{aligned} \tag{3}$$

Here the value α corresponds to the probability of having a faulty pixel in the image. The probability α is typically very low [14]. Figures 1-3 show the effect of Gaussian and Salt and Pepper noise models compared to original image.

Figure 1: Original image.

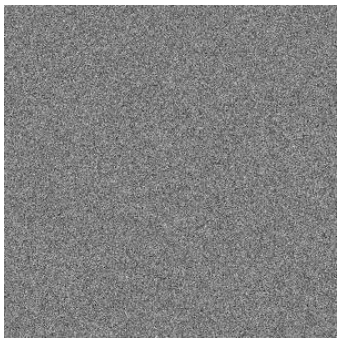

Figure 2: Gaussian noise corrupted image with $\mu = 0$ and $\sigma = 0.1$.

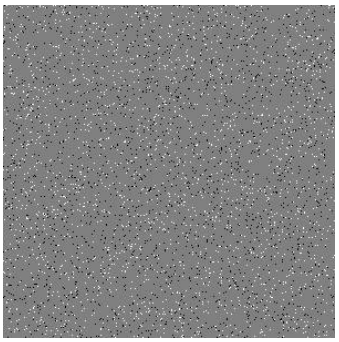

Figure 3: Salt and Pepper noise corrupted image with $\alpha = 0.05$.

2.2 Image data

The image data used in this thesis was captured purely for needs of this study. In total of three different image setups were arranged, and for each

setup, 84 exposures were taken consecutively in order to analyze the methods properly. The images were taken with Nikon D7100 DSLR (digital single-lens-reflective) camera which has a 24-megapixel CMOS-sensor. Due to the high pixel count in the images, the corresponding file sizes tend to be large. Therefore, 84 exposures of each image were taken for maintaining the ability to process and analyze the images relatively efficiently. The three different images are shown in Figure 4.

Figure 4: The three images used in this study.

As noted in the Introduction, one of the disadvantages of multi-image denoising methods is the requirement for stationary subject. In order to accomplish this requirement, the camera setup was designed such that it would minimize movement between separate exposures. One of the most important tools of this demand was a sturdy tripod, which was used in every setup. Another aspect of reducing the camera shake was the use of a wireless remote shutter, which eliminates movement of the camera that might occur while pressing the physical shutter of the camera. In addition to the stationarity of the camera, exposure settings play an important role in obtaining identical images successively. The camera was put to manual exposure settings (shutter speed, aperture and ISO) and manual white balance setting for this purpose. This procedure excludes the possibility of exposure settings to change between shots. Finally, all the images were taken indoors to reduce changes in lighting during taking images. As indoor lighting such as halogen lamps do not provide stable lighting, a smartphone constant flash was used to light the setups.

The images were captured in RAW format, which is lossless format to store image data. Unlike JPEG format, RAW format maintains all data the sensor captures and do not compress the data by any means. Actual RAW data is important in this study, since noise can transform during image file compression done by the camera, when using other formats than RAW. As can be seen from Figure 4, all the images are slightly underexposed. The reason for

capturing darker images is due to the noise being more intensive in dark areas of images. The images were also shot using higher ISO-values (ISO 100-1600) to amplify the noise even more, which is beneficial when comparing different denoising methods. Exposure settings used in each image are listed in Table 1. After capturing the images, they were imported to RStudio. In order to simplify analysis of the noise, the files were converted to greyscale images using R-package 'OpenImageR' [13]. Finally, the greyscale images were saved as data matrices using the package.

Table 1: Exposure settings of the images.

	Image 1	Image 2	Image 3
Shutter speed	1/60 s	1/60 s	1/15 s
Aperture	$f/3.5$	$f/3.8$	$f/5.3$
ISO	1600	1100	100

2.3 Distribution tests

In this section we test the captured image data, aiming to get an idea of what type of noise model does the noise actually resemble. Furthermore, we calculate some interesting characteristics of the observed noise. In order to justify the dominant noise model in the captured images, a few normality tests were performed to find out whether the dominant noise is actually Gaussian noise or not.

Normality of the noise was tested by using an extension of Shapiro and Wilk's W test for normality to large samples [16]. The test was performed by using R function that calculates the test statistics and p-values for the aforementioned test. Testing was done individually for the three images. For each image, 4000 random pixel coordinates (of the 24 million possible) were calculated and the p-value of the test was computed for each 4000 pixels coordinates using the 84 corresponding pixels as a sample. After obtaining the 4000 p-values for each image, the percentage of significantly non-normal pixels was calculated using two different significance levels $(1 - \alpha)$. The corresponding percentages are listed in Table 2. In addition, the corresponding histograms of the p-values are given in Figure 5.

Table 2: Percentages of non-normal pixels on different significance levels ($1-\alpha$).

	Image 1	Image 2	Image 3
$\alpha = 5\%$	16.0 %	23.4 %	7.9 %
$\alpha = 1\%$	6.1 %	12.3 %	2.0 %

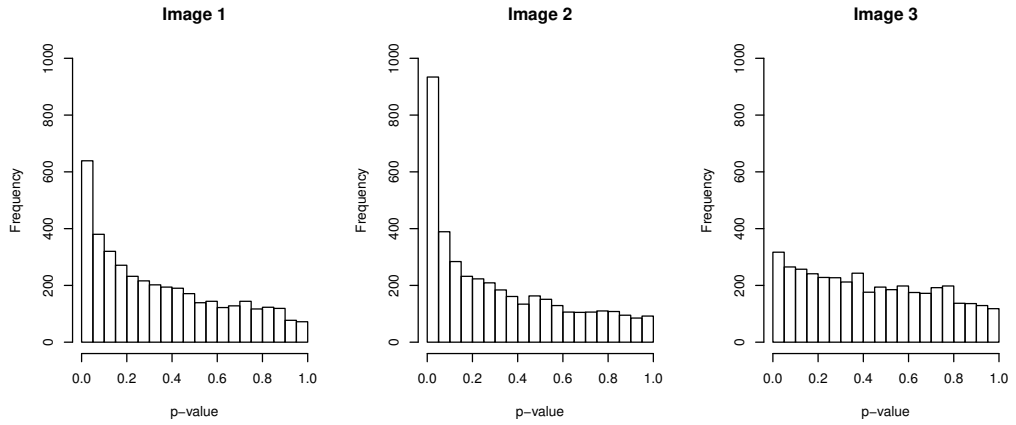

Figure 5: Histograms of p-values for normality test.

Due to the relatively high percentages of the significantly normal noise values of the images, the dominant noise model appears to be quite Gaussian. According to Table 2, the noise in Image 2 was the least normal. As Image 2 is the darkest one, it might be that there is some other noise model more present in darker lighting situations. Another observation from Table 2 is that noise is the most Gaussian in Image 3, which is taken with the lowest ISO-value. ISO-value controls the sensitivity of the sensor. The result thus indicates introduction of other noise models when using higher sensitivity settings of the sensor. Despite the slight non-normality of Image 2, the results yield great applicability of additive and Gaussian noise models in all three images, which suggest the usefulness of multiple image denoising techniques.

Another interesting aspect of the noise is whether it depends on the grey level values of the underlying image $f(x, y)$. To test this hypothesis, variances of the pixels were calculated in both bright and dark areas of the image. In this test, only the Image 1 was considered since it provided very varying grey levels across the image. Bright pixels were considered those with grey level

values in range from 0.7 to 0.9. Similarly, dark pixels were those in range from 0.1 to 0.3. Both the brightest and the darkest values were left out of consideration due to the absence of variance in blown-out pixels. That is, in very bright areas the pixel values might all be at the maximum of 1.0, and the variance should thus be zero. The test was performed by first selecting 1500 bright and dark pixels, as defined above, randomly from Image 1. For each pair of bright and dark pixel, the variance of the corresponding pixel was calculated among the 84 available images. In addition, the variances of the two pixels were compared using Bartlett test, in order to verify whether the variances were the same or not [2]. The results of the variances are shown in Table 3.

Table 3: Variances of bright and dark pixels.

	Bright	Dark
Sum	1.59	1.29
Mean	0.0011	0.0009
Median	0.0007	0.0009

According to the Bartlett test, the variances between bright and dark pixels are different. 60.9% of the 1500 tests resulted in a p-value less than 5%, which suggests rejecting the null hypothesis of equal variances. Thus it can be stated that in general, bright pixels have more noise, in terms of variance. To visualize this result, 500 random pixel coordinates were evaluated from each three images. The variances of these pixels were calculated and plotted as a function of grey level values. The resulting plot is shown in Figure 6.

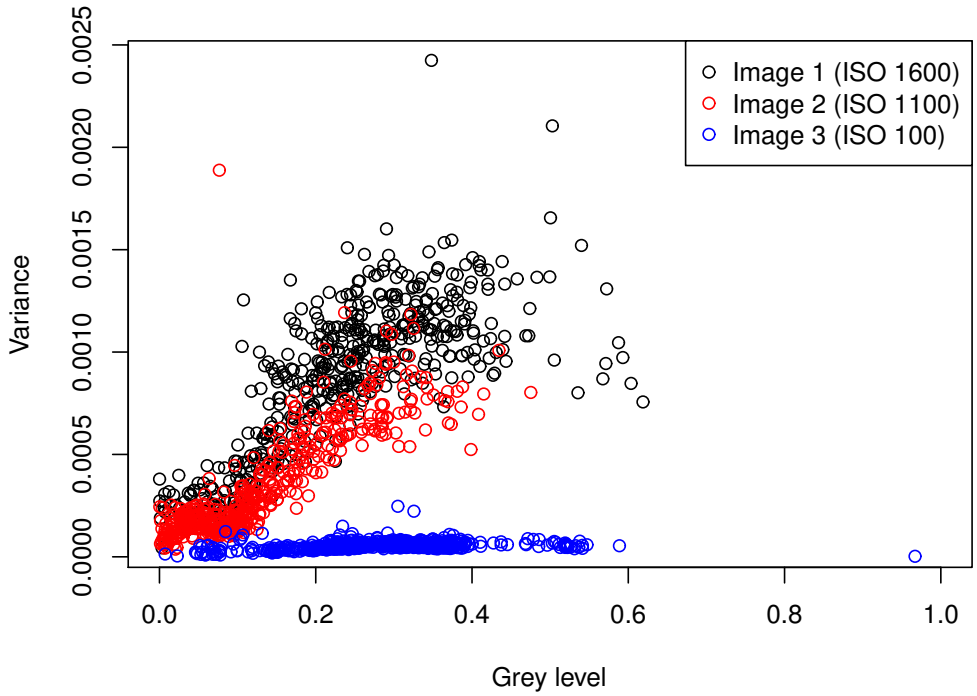

Figure 6: Noise variance as a function of grey level value.

As can be seen from Figure 6, variance of the pixel values, or noise, tends to increase as pixels get brighter, which agrees with the Bartlett test performed earlier. Yet another relatively interesting phenomenon is visible in Figure 6. One of the widely known principles of exposure is that higher sensitivities (ISO-values) result in greater amount of noise. This behaviour is apparent in the figure. Image 1 is taken with ISO 1600 and it introduces roughly ten times more noise compared to Image 3, which is taken with ISO 100. Figure 6 also justifies the fact that all the three images are considerably under-exposed, as the brightest pixels lie somewhere around grey level value of 0.6.

The third, and final noise test was used to examine whether the noise depended on the neighbouring pixel noise or not. That is, it was tested if two adjacent pixels shared the same variance in comparison to two random pixels. The test was executed as follows. A random pair of pixel coordinates were calculated and their variances were compared by using the aforementioned Bartlett test [2], with 95 % significance level. A third random pixel

was compared to its neighbour pixel, which was obtained by adding one to the x-coordinate, thus yielding the right-hand side neighbour. This process was repeated 1500 times and the corresponding Bartlett test p-values were saved into an array. The results are shown as histograms in Figure 7.

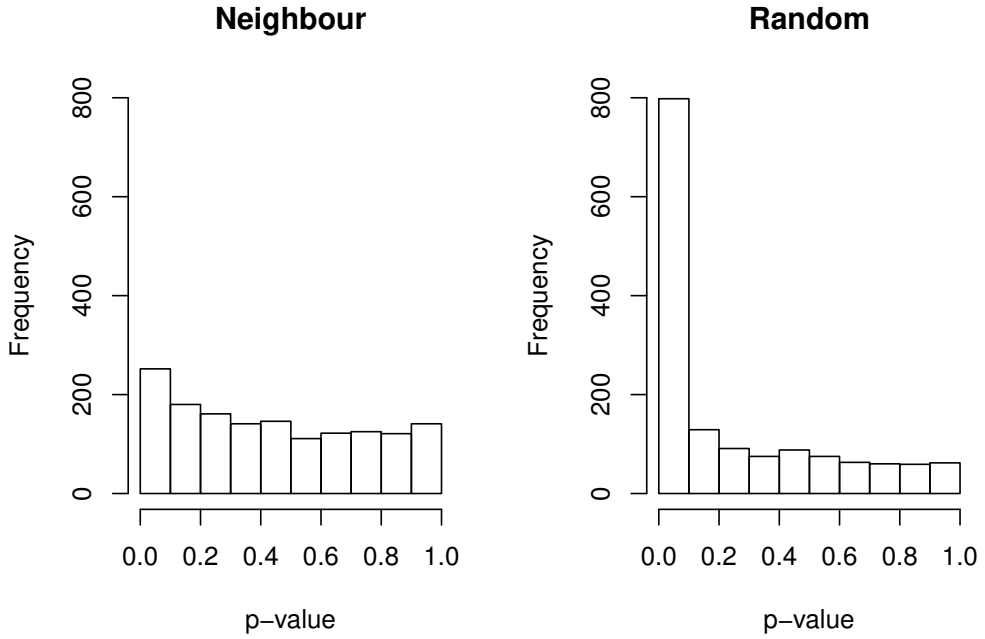

Figure 7: P-values of Bartlett test comparing variances of random and adjacent pixels.

As Figure 7 suggests, the noise appears to be dependent on the noise of its neighbouring pixel. Moreover, 9.7 % of the neighbouring pixels were classified as having unequal variances, according to Bartlett test, whereas the corresponding percentage for random pixels was 47.3 %. This result agrees with the earlier result of the variance dependency on grey levels, as neighbouring pixels typically have similar brightness values.

3 Noise reduction

The fundamental purpose of image noise reduction is to scale down the unwanted noise while preserving information like texture or edges. The motivation for noise reduction, or denoising, might be purely aesthetic or denoising might be first step of image enhancement before use of some other method, such as computer vision. On the other hand, a noisy image was taught to be composed of the real image and the noise, as in the additive model in Equation (1). Noise reduction thus aims to minimize $n(x, y)$, when the additive model is considered. There are a vast number of different noise reduction methods, a few of which are introduced in [14]. Most of these methods considers a single image by attempting to minimize effects of noise in the given image. Along with these conventional single-image denoising methods, there are methods that use information of multiple consecutive exposures and combine these images to obtain one less noisy image. In this section we will introduce two relatively simple multi-image denoising methods and compare them to more traditional ones.

3.1 Conventional noise reduction

There are numerous single-image denoising techniques available. The reason for this is that typically it is not possible to acquire multiple images of the same source. Thus all the information available is limited to the single image. These methods can be sub-categorized based on the domain where the denoising filtering takes place [14]. Spatial domain handles pixel values as they are in the image plane, whereas frequency domain filtering transforms the spatial domain into frequencies, which is sometimes referred to as wavelet domain [11]. In this section, we will concentrate on the simpler spatial domain methods. The methods of interest are one of the most widely known ones. We will introduce two methods, or filters, which are linear smoothing filter and non-linear smoothing filter, both of which we will compare with the multi-image methods in Section 4.

The linear smoothing filter reduces noise by averaging neighbouring pixels using a square convolution mask [5]. The mask, or window, is used to replace the center pixel with a weighted sum of pixel values within the mask area. The mask is shifted across each pixel in the image and the center pixel is replaced by the obtained value. The size of the mask is typically from 3×3 to 7×7. The bigger the mask area is, the more noise reduction is applied.

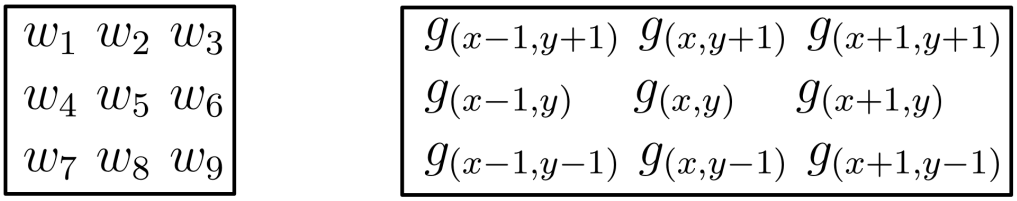

Figure 8: Linear spatial smoothing weights and mask.

Figure 8 illustrates the weight distribution and mask when the new pixel value is calculated for pixel (x, y). The windows size used in Figure 8 is 3×3. The new value for the center pixel, $c(x, y)$, is thus calculated as

$$\begin{aligned} c(x,y) =& w_1 g_{(x-1,y+1)} + w_2 g_{(x,y+1)} + w_3 g_{(x+1,y+1)} \\ &+ w_4 g_{(x-1,y)} + w_5 g_{(x,y)} + w_6 g_{(x+1,y)} \\ &+ w_7 g_{(x-1,y-1)} + w_8 g_{(x,y-1)} + w_9 g_{(x+1,y-1)}. \end{aligned} \tag{4}$$

In a pure mean filter, the weights in Figure 8 are all equal and their sum is 1, which ensures that the overall brightness of the image is preserved. As the mask considers adjacent pixel values from all directions of the center pixel, image borders have to be handled separately. There are a couple of ways to treat the border. One option is to duplicate the pixel values closest to border and place them beyond the image area. Another approach is to assign zero weights to those pixels outside the image margins. In this case, the remaining weights have to be scaled so that the sum of the weights remains constant.

The result of linear spatial smoothing filtering is visible noise reduction and smoothing. However, as the filter takes averages of the neighbouring pixels, it can be seen as a type of low-pass filter, since the procedure reduces intensity variations within the mask area. While the noise is significantly reduced, edges and other sharp features of the images are also blurred. Due to these side effects, such as the edge blurring, more sophisticated methods have been developed to prevent this issue. For example, the above-mentioned frequency domain denoising methods as well as multi-image methods are superior in preserving features [14, 17].

The linear spatial smoothing filter is relatively good for handling Gaussian noise. However, in some cases non-linear smoothing filters might be more applicable. A widely known example of a non-linear filter is the median filter.

Spatial median filter is implemented as the linear smoothing filter, but the center pixel is replaced by the median value of the pixels within the mask. Median filter is considered the best performing order statistic filter, since it is very good at eliminating extremely distinctive noise values in an image. Due to the quality of removing extreme values, median filter is exceptional for removing Salt and Pepper noise [17].

3.2 Merging methods

In this section we introduce two important multi-image noise reduction methods, which merges together multiple images. These methods utilize the additional information provided by different exposures, in order to reduce noise efficiently. The methods to be covered are called image averaging method and median method. Both of these techniques are relatively simple to implement, yet they are very powerful methods in certain situations.

Image averaging over multiple consecutive frames is widely known technique for attaining noise-reduced images. Image averaging is also a very intuitive way of reducing random variations between different exposures. In addition, the method is often used as a preprocessing action on various image enchantment algorithms when multiple frames are available [7]. On the other hand, image averaging can be employed even in applications where only a single image is considered, as a process to merge phases of more advanced image denoising techniques [12].

Image averaging is a straightforward method. The noise-reduced image is obtained by taking averages of the N available images pixel-wise. That is, each pixel in the resulting image is obtained by taking the mean of all the pixel values corresponding to the same spatial location to that pixel [10]. Before the method can be applied, the images must be aligned to prevent blurry results. The data used in this study was acquired such that there is no need for further alignment, as described in Subsection 2.2.

The idea behind image averaging is based on the additive model (1). The resulting image, denoted here by $G(x, y)$, is obtained by taking the average of the N images, that is

$$G(x, y) = \frac{1}{N} \sum_{i=1}^{N} g_i(x, y). \tag{5}$$

Since the image can be decomposed into two parts, the denoised image can be expressed in terms of the underlying image $f(x, y)$ and the noise $n(x, y)$,

$$G(x, y) = \frac{1}{N} \sum_{i=1}^{N} f_i(x, y) + \frac{1}{N} \sum_{i=1}^{N} n_i(x, y). \tag{6}$$

Because the underlying image $f(x, y)$ is constant, $G(x, y)$ can be written as

$$G(x, y) = f(x, y) + \frac{1}{N} \sum_{i=1}^{N} n_i(x, y). \tag{7}$$

From Equation (7) it is visible that averaging multiple images reduce the noise term $n(x, y)$ as it tends closer to its mean, which is assumed to be zero. Due to the law of large numbers, increasing the number of averaged images causes the noise term to disappear [9, 8]. As this result suggests, image averaging can be very effective noise reduction method when its assumptions hold. The image data used in this thesis is mostly corrupted with Gaussian noise. Since Gaussian noise obeys the additive model fairly well, there is a reasonable change that image averaging works very well for the test data. One of the advantages of image averaging method is the great ability to preserve actual details of the image. Since the method does not consider the neighboring pixel values at all, image averaging can maintain edges up to one pixel wide, whereas the aforementioned filtering techniques will always soften edges that narrow. Visual comparison between the methods is performed in Section 4.

Another multi-image noise reduction method is the median technique. Like image averaging, median method is a pixel-wise merging procedure that is also remarkably applicable in some situations. As the name suggests, median method replaces each pixel in the resulting image by taking the median of all the N grey level values that share the same pixel coordinates. This technique is powerful for removing strong deviations from the captured images. Due to the robustness of this method, median is particularly effective of removing Salt and Pepper noise that is present in some of the merged images. The reason for efficient Salt and Pepper noise removal is the low probability of corrupted pixels, as discussed in Subsection 2.1. The probability that a corrupted pixel is observed is α. For merging three images together thus requires two corrupted pixels among the three, both having either the maximum or minimum value. The probability of having two corrupted pixel of the same value is then $\binom{3}{2}(\frac{\alpha}{2})^2$. Since the corrupted value can be either minimum or

maximum, the probability has to be multiplied by two. Finally, the probability of preserving Salt and Pepper noise, after median method is applied for three images, is $2\binom{3}{2}(\frac{\alpha}{2})^2$. For a typical value of $\alpha = 0.05$, the probability is then 0.4%. This yields remarkably good performance for removing Salt and Pepper noise in the resulting image, since the probability further decrease as the number of merged images is increased.

Both of the methods introduced in this section were implemented in R, using the package 'OpenImageR' [13]. The image data was manipulated as matrices and the merged matrices were exported back to image files using the package.

4 Analysis of different methods

In this section we test the noise reduction methods in action, using the acquired data. Traditionally, image noise reduction methods are tested and compared by simulating artificial noise on top of noise-free test images. The methods are then compared by calculating statistics, such as signal-to-noise ratios, to determine which methods come closest to the noise-free image [3, 12, 17]. In this study, however, the image data is already noise-contaminated, as the images were taken with a regular consumer camera. That is, no additional noise is generated to the images, but the existing noise is to be removed by applying the introduced methods. Since the underlying noise-free image of the test images is unknown, the comparison are performed by analyzing the variance that is left present after the method has been employed on a set of images. This comparison method is based on the assumption that the variance among the test images is the closer to zero the closer the noise-reduced image is to the underlying noise-free image. In addition to this more quantitative comparison approach, each of the methods are assessed by visual perception, as visual enchantment is often the motivation for noise reduction. In the following section, both the single-image and multi-image methods are used to reduce noise from the test images and the methods are later compared. For the spatial filtering methods, a 5×5 mask size was used. Similarly, the multi-image methods were applied using five image average or median. The reason for the use of larger mask and higher number of images is the more visible differences between the methods.

4.1 Noise reduction

We begin with the more conventional single-image methods. Since the multi-image methods combine five exposures into one image, only one fifth of the images were processed with the single-image methods. The reason for this is the ability to compare the conventional methods to the multi-image counterparts. In order to compare the methods reliably, the image to be processed was picked randomly among the five images used in multi-image methods. Thus every method yields 16 resulting images per image setup (e.g. Image 1). As described above, the tests were based on pixel variance across the processed images. For each image setup, 1500 random pixel coordinates were computed and the variances of these pixels were analyzed among the 16 processed images for each method. Figure 9 shows the distribution of the calculated 1500 pixel variances of the original images and the images processed with the single image methods, spatial averaging and spatial smoothing filters, respectively. The image used in Figure 9 is Image 1, due to the large amount of noise in the image. As can be seen from Figure 9, both single-image methods reduce noise remarkably well, in terms of decreased variance. Judging by the variance, average filter appears to be slightly more effective. Figure 10, on the other hand, shows the visual effect of the methods. The image used in this figure is Image 2 and it is cropped to 300×300 pixels so that the effects are easily visible. Again, by looking at Figure 10, both methods reduce noise effectively. The spatial smoothing behaviour is also visible, since the edges of the images are smoothed and the texture of the fabric is less detailed. Both figures suggest that the averaging method might be slightly better method for reducing noise, considering the smaller variance and smoother surface in Figure 10.

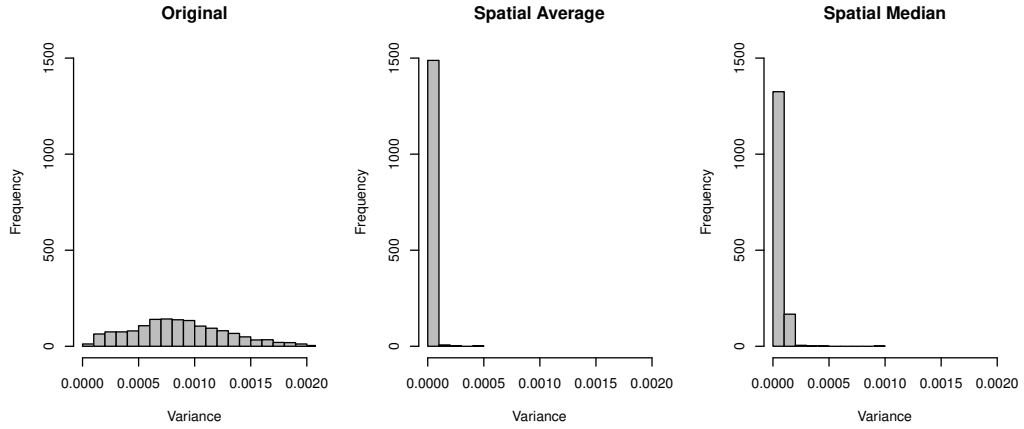

Figure 9: Variance on Image 1 after applying spatial smoothing filters.

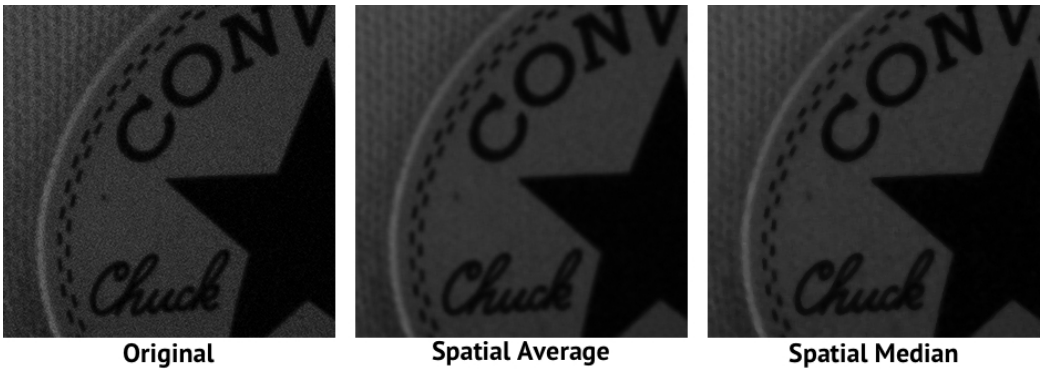

Figure 10: The effect of spatial smoothing filters on Image 2.

The tests were performed similarly for the multi-image denoising methods. One distinction to the single-image methods was that instead of picking images randomly, all of the five images were merged together. Thus, this method provided 16 images per image setup. Corresponding figures were plotted for the merging methods as well. Figure 11 shows the variances calculated from Image 1 for each method. The variance is again smaller in both methods compared to the unprocessed image. Even though the result is less effective compared to the single-image ones, the difference to the original image is obvious. This time, averaging seems to be significantly better than median method. The undeniable advantages of the merging methods are clearly vis-

ible in the Figure 11. The noise is reduced by vast amount, yet the features of the image, like the text and the stitches of the badge, are well preserved. While both the averaging and median perform sufficiently well, the averaging method outperforms the median method by some degree. In Subsection 4.2, we compare the results of each method by means of variance as well as visual properties. We also test how well the methods affect the different image setups, given the various exposure settings, like sensitivity.

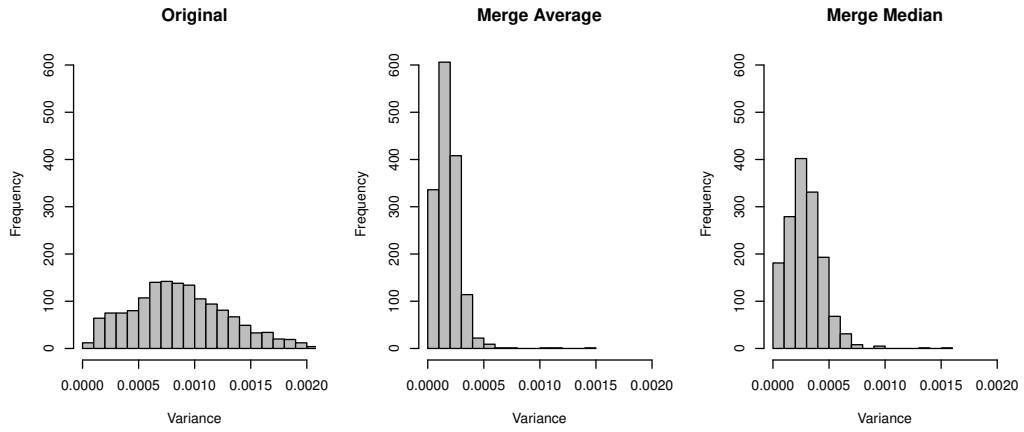

Figure 11: Variance on Image 1 after applying merging methods.

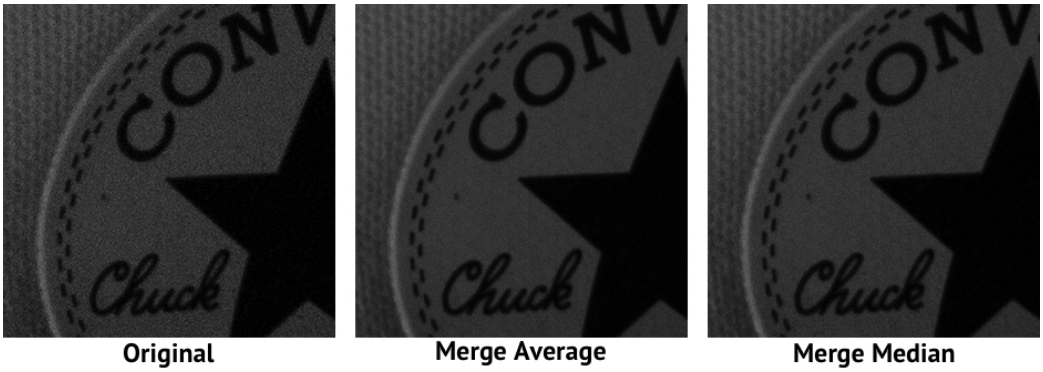

Figure 12: The effect of merging methods on Image 2.

4.2 Comparison of the applied methods

All applied methods are capable of reducing unwanted noise from the test images. Now we concentrate on the differences of these methods, emphasizing the differences between the single-image and multi-image methods. We keep on analyzing the variances left in the images after applying the methods. Since 1500 random pixel variances were calculated from each image and for each method, we have total of 4500 variance measurements per method, corresponding to all three images. Some descriptive statistics of these variances are collected into Table 4. Similar conclusions can be drawn from Table 4 as from Figures 9 and 11. The variability among the pixels decreases in all the methods applied on the test images. It can be seen as well that the spatial single-image methods reduce the noise by greater extent in terms of variance. In addition, averaging versions of the methods seem to exceed the median ones across all the statistics, which indicates better performance for averaging methods at least for the test data used in this study.

Table 4: Variance across images after different methods applied.

	Original	Spatial Average	Spatial Median	Merge Average	Merge Median
Sum	1.9	0.086	0.15	0.39	0.62
Mean $[10^{-4}]$	4.2	0.19	0.33	0.87	1.4
Median $[10^{-4}]$	2.1	0.14	0.20	0.45	0.64

Figure 13 illustrates the variance present in the processed images as well as the effect of the methods on different images and sensitivity levels. In Figure 13, only the averaging methods have been taken into consideration with the original image, since the results between average and median are very similar. Furthermore, in order to simplify the plot, only 900 values of the 4500 have been randomly chosen per image setup. The placement of the data points along x-axis is arbitrary except the arrangement into image categories. The conclusions drawn from Figure 13 coincides with the conclusions made earlier. Spatial filter produces better noise reduction results compared to merging method, variance-wise. However, Figure 13 provides evidence for the stability of the order between different images. Particularly, the spatial filter appears to be the best option in all three images, being significantly superior on decreasing noise. As Figure 13 suggests, it seems that the methods are considerably independent on the sensitivity of the sensor and thus the intensity of the noise. In order to further examine this hypothesis we calculate percentages of the variances to see how much noise there is left after the

methods have been employed. Table 5 shows the percentages of the variance that is left in the test images compared to the original variance. According to Table 5, the effectiveness of the methods is remarkably independent of the noise strength. Especially the merging methods appear to obey this hypothesis well, whereas the spatial methods tend to perform better on higher sensitivities (or noise levels).

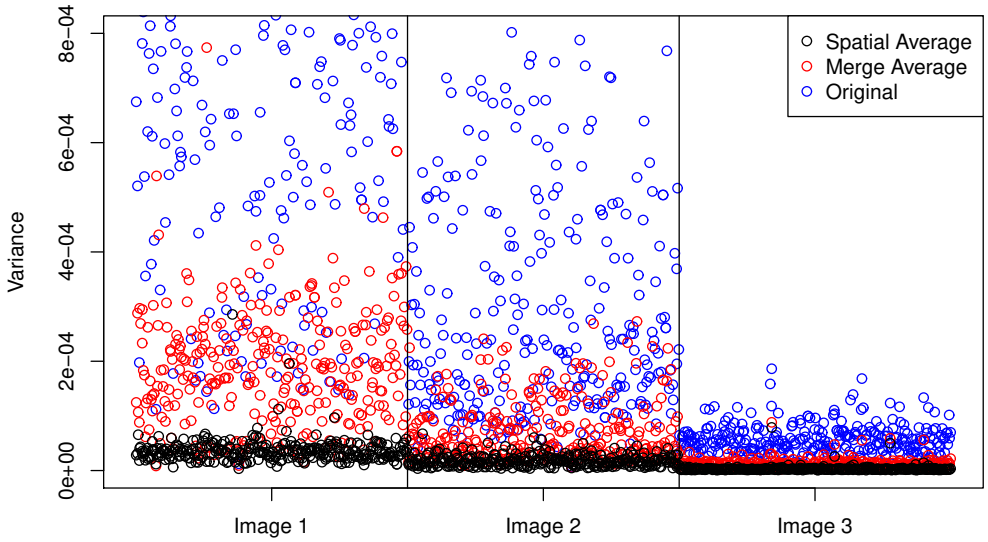

Figure 13: The effect of methods on different images.

Table 5: Variance left in images after methods applied.

	Original	Spatial Average	Spatial Median	Merge Average	Merge Median
Image 1 [%]	100	4.1	7.4	21	32
Image 2 [%]	100	5.4	8.5	21	31
Image 3 [%]	100	5.5	9.7	21	32

In terms of variance in the resulting images, the spatial single-image methods provide a better outcome for noise reduction. However, the purpose of noise reduction is essentially on the visual side. Hence, it is at least equally important to compare the visual effects of the methods. Figures 10 and 12 indicated both pleasing visual results for reducing the apparent noise in the

original test image. In Figure 14 we have emphasized the differences of the methods. Figure 14 shows a 300×300 crop of the Image 1 with each method applied.

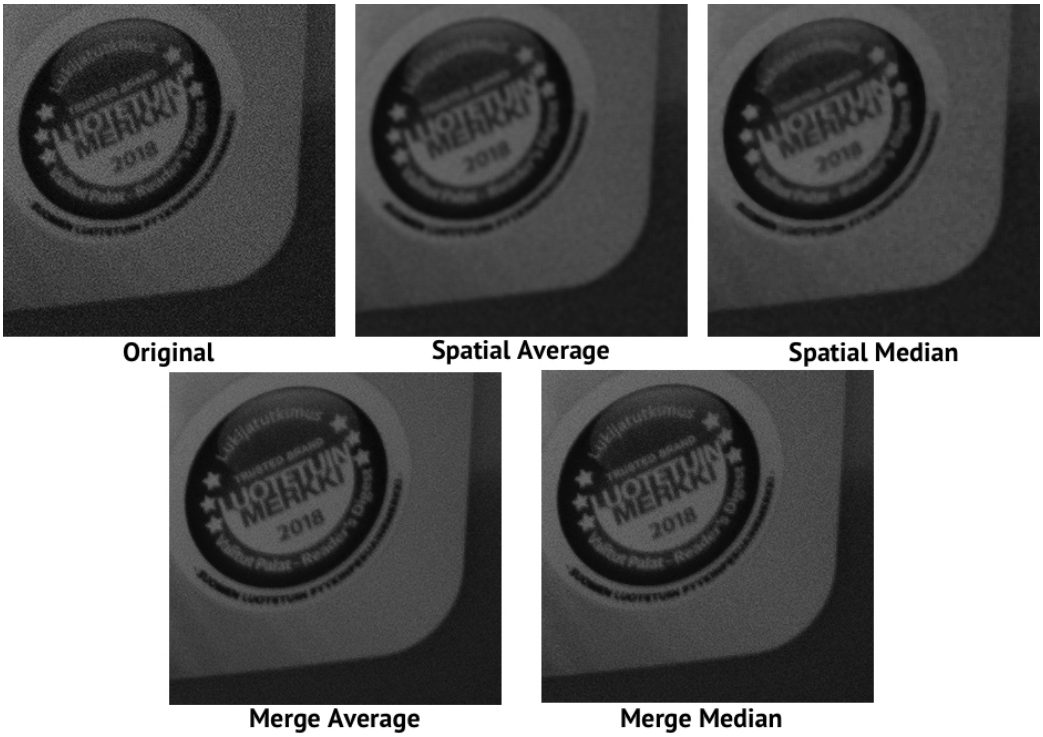

Figure 14: The effect of each method on Image 1.

From Figure 14 it is again obvious that each method manage to reduce noise in visual manner. This can be best seen by examining the light grey surface above the badge. Both merging methods produces even surface with almost indistinguishable noise left in the images. The little noise visible in the merging method images looks similar to the original image, but with less intensity. On the other hand, the spatial methods seem to have modified the structure of the noise. Particularly, the noise grains are visibly larger compared to the original image or merge processed images while the intensity has decreased. This is most probably due to the fact that spatial methods include values from neighbouring pixels as well, with a filter of size 5×5, in this case. The same effect is also visible in Figure 10, where the flat surface shows similar grain noise. By analyzing the even gray surface in Figure 14 further, it can be stated that the noise reduction performs better using the averaging alternative of both spatial and merging methods. However, the superiority of the

averaging versions only applies for the test data, which was earlier considered to be corrupted by mainly Gaussian noise. The results might be better for median methods for some other test images or setups.

Figure 14 also provides excellent opportunity to compare the feature preserving properties of the methods. The disadvantages of these smoothing filters are definitely visible, when comparing the spatial methods to the original image. The text in the badge is blurred and the hard edges between the differently colored areas are smoother. Overall, both images processed with spatial methods are blurred and less detailed compared to the original. For the merged images in Figure 14, however, the feature preserving properties are apparent. The edges are sharp and the text is legible throughout the images. The sharpness of the merged images is even greater compared to the unprocessed image, which can be justified by looking at the undermost text in the badge. The text is more detailed in the merged images. This result is one of the biggest advantages of using image merging methods for noise reduction purposes.

5 Conclusions

In this thesis, we have studied several noise reduction techniques for removing noise from photographs taken with a standard consumer DSLR camera. The aim was to compare multiple image merging methods to some conventional denoising algorithms that only process single images. Before the methods were applied, the noise of the test images was analyzed. The tests suggested that the test images were mostly degraded by additive Gaussian noise, which is desirable taking into account the additive nature of the noise reduction methods employed in this thesis. The merging methods were tested along with the conventional ones by analyzing the remaining noise and the visual properties of the processed images. The experiments indicated very applicable performance for the multi-image averaging method, with the median alternative not far behind. While the conventional single-image methods considered in this thesis were very elementary, the potential of merging methods proved to be significant compared to single-image methods. One must keep in mind, though, that the state-of-the-art single-image methods are extremely effective and they might outperform these merging methods. However, the leading modern noise reduction methods utilize rather complex procedures such as wavelet transforms and AI. In contrast, the proposed merging methods are really simple to implement.

Due to the advantages and disadvantages, merging methods turn out to be suitable for applications such as astrophotography, landscape photography or medical imaging. The reason for the narrower field of applications proved obvious in this thesis. The test setups were rather sensitive to changes in lighting or movement, when acquiring the test data. However, when these restrictions can be overcome, the results are pleasant. In this study, we merged together five consecutive images, which yielded notable reduction in the noise. The number of images to be merged is not limited, though. Figure 15 shows the behaviour of noise when more images are averaged. From Figure 15 it is visible, that improvement can still be made, from eight images, all the way to 20 merged images.

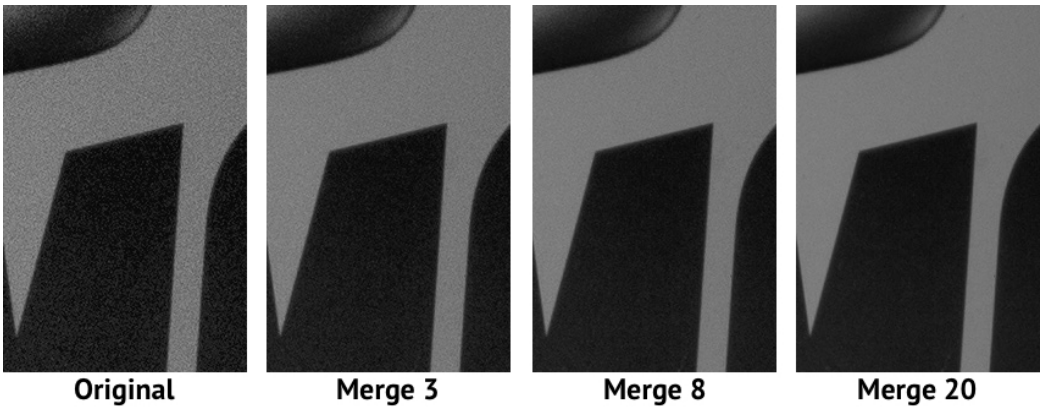

Figure 15: Example of increasing the number of images to be averaged.

In this thesis we found out that the averaging approach provided slightly better results compared to the median approach. However, this observation is highly correlated with the test data. For example, it is known that the median is superior of removing Salt and Pepper noise. This emphasizes the importance of choosing the right noise reduction technique for specific noise type. Particularly, the results in this thesis suggest choosing the averaging alternative over median, if the images are taken with a consumer DSLR camera, that features a CMOS-sensor.

The objective of this thesis was to compare the benefits of multiple image noise reduction methods to traditional noise reduction techniques. The approach to this objective was to concentrate on the visual performance and purely noise reduction in terms of variance. The analysis of the methods could be expanded to include more theoretical comparisons. This could be

done by generating theoretical noise on top of noise-free images and comparing statistics of the remaining noise, such as signal-to-noise ratio, which is a relatively standard tool in signal processing. In future research, the merging methods could also be compared with the more complex modern noise reduction algorithms in order to justify the use of merging methods over other methods.

References

[1] A. O. Akyüz and E. Reinhard. Noise reduction in high dynamic range imaging. *Journal of Visual Communication and Image Representation*, 18(5):366–376, 2007.

[2] M. S. Bartlett. Properties of sufficiency and statistical tests. *Proceedings of the Royal Society of London. Series A-Mathematical and Physical Sciences*, 160(901):268–282, 1937.

[3] A. C. Bovik. *Handbook of image and video processing*. Academic press, 2010.

[4] A. K. Boyat and B. K. Joshi. A review paper: noise models in digital image processing. *arXiv preprint arXiv:1505.03489*, 2015.

[5] A. Buades, B. Coll, and J-M Morel. A non-local algorithm for image denoising. In *2005 IEEE Computer Society Conference on Computer Vision and Pattern Recognition (CVPR'05)*, volume 2, pages 60–65. IEEE, 2005.

[6] T. Buades, Y. Lou, J-M Morel, and Z. Tang. A note on multi-image denoising. In *2009 International Workshop on Local and Non-Local Approximation in Image Processing*, pages 1–15. IEEE, 2009.

[7] S. G. Burgiss and S. G. Goodridge. Multiframe averaging and homomorphic filtering for clarification of dark and shadowed video scenes. In *Enabling Technologies for Law Enforcement and Security*, volume 4232, pages 480–488. International Society for Optics and Photonics, 2001.

[8] T. S. Ferguson. *A course in large sample theory*. Routledge, 2017.

[9] B. V. Gnedenko. *Theory of probability*. Routledge, 2018.

[10] R. C. Gonzalez and P. Wintz. Digital image processing(book). *Reading, Mass., Addison-Wesley Publishing Co., Inc.(Applied Mathematics and Computation*, (13):451, 1977.

[11] M. Kazubek. Wavelet domain image denoising by thresholding and wiener filtering. *IEEE Signal Processing Letters*, 10(11):324–326, 2003.

[12] J. Luo, Y. Zhu, and I. E. Magnin. Denoising by averaging reconstructed images: Application to magnetic resonance images. *IEEE transactions on biomedical engineering*, 56(3):666–674, 2009.

[13] L. Mouselimis. OpenImageR package documentation, 2019.

[14] J. Patil and S. Jadhav. A comparative study of image denoising techniques. *International Journal of Innovative Research in Science, Engineering and Technology*, 2(3):787–794, 2013.

[15] D. Ratledge. *Digital Astrophotography: The State of the Art*. Springer Science & Business Media, 2006.

[16] J. P. Royston. An extension of shapiro and wilk's w test for normality to large samples. *Journal of the Royal Statistical Society: Series C (Applied Statistics)*, 31(2):115–124, 1982.

[17] R. Verma and J. Ali. A comparative study of various types of image noise and efficient noise removal techniques. *International Journal of advanced research in computer science and software engineering*, 3(10), 2013.